Evaluation of Lipopolysaccharide Aggregation by Light Scattering Spectroscopy

Nuno C. Santos,*[a] Ana C. Silva,[a] Miguel A. R. B. Castanho,[b, c] J. Martins-Silva,[a] and Carlota Saldanha[a]

Lipopolysaccharides (LPS) are cell wall components of Gram-negative bacteria. These molecules behave as bacterial endotoxins and their release into the bloodstream is a determinant of the development of a wide range of pathologies. These amphipathic molecules can self-aggregate into supramolecular structures with different shapes and sizes. The formation of these structures occurs when the LPS concentration is higher than the apparent critical micelle concentration (CMC_a). Light scattering spectroscopy (both static and dynamic) was used to directly characterize the aggregation process of LPS from Escherichia coli *serotype 026:B6. The results point to a CMC_a value of 14 $\mu g\,mL^{-1}$ and the existence of premicelle LPS oligomers below this concentration. Both structures were characterized in terms of molecular weight (5.5×10^6 and $16 \times 10^6\,g\,mol^{-1}$ below and above the CMC_a, respectively), interaction with the aqueous environment, gyration radius (56 and 105 nm), hydrodynamic radius, (60 and 95 nm) and geometry of the supramolecular structures (nearly spherical). Our data indicates that future in vitro experiments should be carried out both below and above the CMC_a. The search for drugs that interact with the aggregates, and thus change the CMC_a and condition LPS interactions in the bloodstream, could be a new way to prevent certain bacterial-endotoxin-related pathologies.*

KEYWORDS:

aggregation · bacteria · light scattering spectroscopy · lipopolysaccharide · supramolecular chemistry

Introduction

Lipopolysaccharides (LPS), cell wall components of Gram-negative bacteria, behave as bacterial endotoxins and determine the development of a wide range of pathologies. During an infection, these pathologies result from LPS release into the blood stream, which leads to fever, flush, diarrhea, inflammation, altered metabolic utilization of substrates (glucose, fatty acids, and aminoacids), impaired microcirculation, and, in some situations, hemorrhage, collapse, shock, coma, and death.[1] LPS molecules (Figure 1) consist of three components (for a review see, for example, Rietschel et al.[2]): lipid A (a phosphoglycolipid responsible for LPS toxicity, immunomodulation, and insertion into a membrane or micelle), a core region (a structurally conserved hetero-oligosaccharide), and the O-specific chain (a highly variable polysaccharide that acts as an important surface antigen). Despite extensive knowledge about LPS molecular structure and the biomedical relevance of the solubility of LPS in an aqueous environment, little is known about the aggregation behavior of LPS molecules.

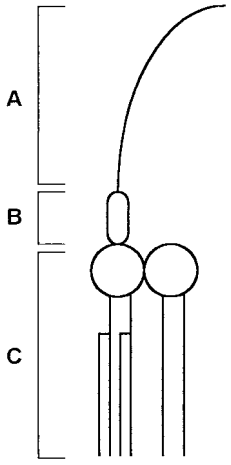

Figure 1. *Schematic representation of the molecular structure of a lipopolysaccharide. A: O-specific chain. B: Core region. C: Lipid A.*

In dilute solution, amphipathic molecules such as LPS usually act as normal solutes and occur as monomers. However, at fairly well-defined concentrations, abrupt changes take place in several physical properties, such as osmotic pressure, turbidity, electrical conductance, and surface tension.[3] The rate at which osmotic pressure increases with concentration becomes abnormally low and the rate of increase in turbidity with concentration is enhanced, which suggests that considerable association is taking place. Moreover, the association usually results in organized aggregates (micelles). The concentration above which micelle formation becomes appreciable is termed the critical micelle concentration (CMC). Simple micelles have lipophilic hydrocarbon chains oriented towards the core and hydrophilic groups in contact with the aqueous medium. Aggregation can

[a] *Prof. N. C. Santos, A. C. Silva, Prof. J. Martins-Silva, Prof. C. Saldanha*
Instituto de Bioquímica/
Instituto de Medicina Molecular
Faculdade de Medicina de Lisboa
Av. Prof. Egas Moniz, 1649-028 Lisboa (Portugal)
Fax: (+351) 2179-3979-1
E-mail: nsantos@fm.ul.pt

[b] *Prof. M. A. R. B. Castanho*
Centro de Química Física Molecular
Complexo I, Instituto Superior Técnico
Av. Rovisco Pais, 1049-001 Lisboa (Portugal)

[c] *Prof. M. A. R. B. Castanho*
Departamento de Química e Bioquímica
Faculdade de Ciências da Universidade de Lisboa
Campo Grande, C8, 1749-016 Lisboa (Portugal)

 © 2003 WILEY-VCH Verlag GmbH & Co. KGaA, Weinheim 1439-4227/03/04/01 $ 20.00+.50/0 ChemBioChem **2003**, 4, 96 – 100

also lead to the formation of different types of larger lamellar structures. Intermolecular attraction between carbon chains as well as minimal contact between carbon chains and aqueous solvent, are responsible for the stabilization of these aggregates. The size and shape of the aggregates depend on the size, shape, and molecular interactions of the constituent monomers. Typically, micelles and lamellar structures tend to be approximately spherical over a fairly wide range of concentrations above the CMC, but there are often marked transitions to larger, nonspherical liquid-crystal structures, mainly at high concentrations.

Knowledge about the micellar behaviour of natural amphipathic molecules such as lipid derivatives is crucial to an understanding of the structural dynamics of living cells and organelles. The free energies of transition between micellar phases tend to be small and, consequently, the phase diagrams for these systems tend to be complex and sensitive to additives.[3] Micelle formation is of practical importance in the formulation of pharmaceutical and other products that contain water-insoluble components, and in detergency, emulsion polymerization, and micellar catalysis of organic reactions.

Critical micelle concentrations can be determined by measuring any micelle-influenced physical property as a function of surfactant concentration. Surface tension, electrical conductivity, and dye solubilization are among the most popular.[4] However, light scattering techniques are far more powerful because information concerning the sizes and shapes of micelles is obtained,[5, 6] as well as more accurate CMC determinations than with other techniques[7].

In the build-up from surfactant monomers to micelles, the transitory existence of intermediate levels of aggregation is to be expected. The existence of submicelle aggregates is possible, although in trace amounts in some cases.[3] Apparent critical micelle concentrations (CMC_a) can be detected in other cases, and premicelle oligomers have been studied both from the experimental and theoretical points of view.[8] However, the role of such structures in biological systems is yet unknown.

The main objective of the present work was to study the physical properties of the process of aggregation in supramolecular structures of the LPS from *Escherichia coli* serotype 026:B6 in Dulbecco's phosphate buffered saline (PBS; pH 7.4). This study was carried out by light scattering spectroscopy techniques (both static and dynamic light scattering), which enabled 1) calculation of the apparent critical micelle concentration, 2) evaluation of the possible existence of LPS premicelle oligomers, and 3) evaluation of the shape, size distribution, average molar weight, average gyration radius, and average hydrodynamic radius of the LPS monomers (or premicelle oligomers) and micelles, below and above the CMC_a, respectively.

Results

The standard CONTIN method[9] allows both calculation of the average hydrodynamic radius (or diameter) and determination of the size distribution of the sample under evaluation. Figure 2 presents the size distribution obtained for one of the studied concentrations of lipopolysaccharide from *Escherichia coli* serotype 026:B6 (80 μg mL^{-1}) in Dulbecco's PBS (pH 7.4) at 37 °C. The broadness of the sample size distributions was quantified by using the polydispersion index calculated by the method of cumulants.[10] The values obtained for the different LPS concentrations under evaluation are presented in Figure 3. The lowest

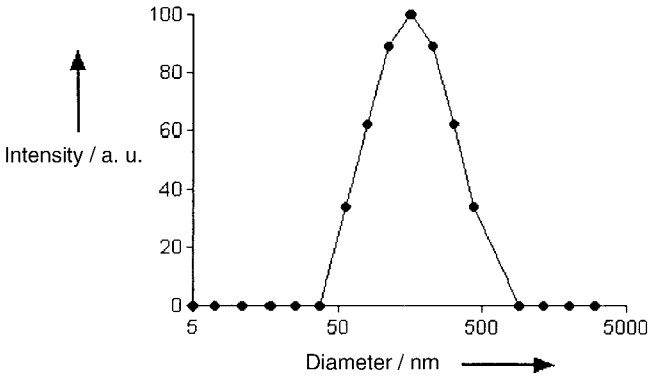

Figure 2. *Size distribution obtained for the LPS aggregates by dynamic light scattering by using the CONTIN method (c = 80 μg mL^{-1}; θ = 90°).*

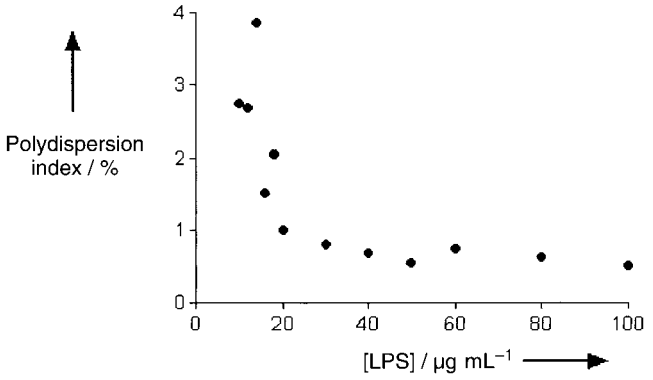

Figure 3. *Polydispersion indexes obtained by dynamic light scattering and the method of cumulants at different LPS concentrations.*

polydispersion indexes were obtained at the higher LPS concentrations, which points to the formation of organized supramolecular systems. Polydispersion is higher close to 14 μg mL^{-1} (this parameter typically increases in the region of the apparent critical micelle concentration). The polydispersion index ranges from 3.86% at 14 μg mL^{-1}, to 0.49% at 100 μg mL^{-1}.

The variation of the maxima of the size (hydrodynamic diameter) distributions obtained by dynamic light scattering (DLS) with LPS concentration as found by the CONTIN method is presented in Figure 4. The lower limit of the transition region in this distribution can be used to calculate the apparent critical micelle concentration and gives a value of approximately 14 μg mL^{-1}, in agreement with the polydispersion data. There was no significant scattering angle (θ) dependence of the DLS results. Additional use of the Debye method, as described in the Methods section, further confirmed an apparent critical micelle concentration value of 14 μg mL^{-1}.

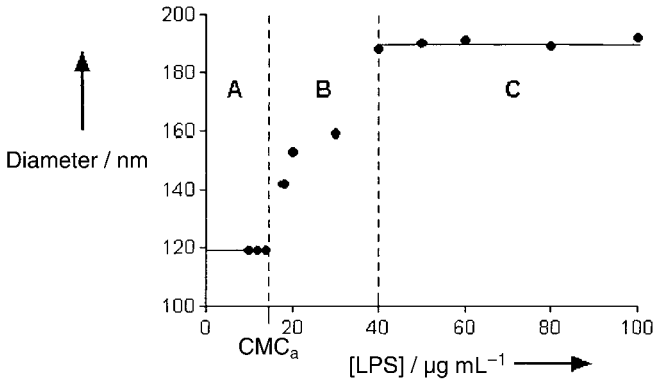

Figure 4. *Variation of the maxima of the size distributions (hydrodynamic diameter) obtained by dynamic light scattering by using the standard CONTIN method. The two horizontal lines represent the average hydrodynamic diameters of the premicelle oligomers (119 nm) and large aggregates (190 nm). The two vertical dashed lines define three concentration regions: A) only premicelle oligomers are present; B) transition range; the coexistence of premicelle oligomers and larger aggregates leads to apparent intermediate diameters as a result of the balance of the light scattering contributions from the two supramolecular species in the calculations of the diameter; C) the light scattering information arises (almost) exclusively from the larger aggregates.*

The values obtained by static and dynamic light scattering for all the different parameters under evaluation—molecular weight (M_w), second virial coefficient (A_2), gyration radius (R_g), hydrodynamic radius (R_h), and ρ—below and above the CMC$_a$, are presented in Table 1.

Table 1. *Values obtained by light scattering spectroscopy for the various parameters under evaluation, below and above the apparent critical micelle concentration.*[a]

	$c < \text{CMC}_a$	$c > \text{CMC}_a$
$M_w/10^6$ [g mol^{-1}]	5.5 ± 0.6	16.0 ± 1.6
$A_2/10^{-4}$ [cm^3 mol g^{-2}]	-42.8 ± 2.1	-0.68 ± 0.03
R_g [nm]	56 ± 7	105 ± 13
R_h [nm]	60 ± 3	95 ± 5
$\rho = R_g/R_h$	0.86 ± 0.11	1.10 ± 0.14
CMC$_a$ [μg mL^{-1}]	14	

[a] Measurements were made on the lipopolysaccharide from *Escherichia coli* serotype 026:B6 at 37 °C in PBS (pH 7.4). Error boundaries given are the typical standard deviation.

Discussion

To the best of our knowledge, this work presents the first direct characterization of the physical properties of the aggregation process of the LPS from *E. coli* serotype 026:B6. It is also the first aggregation process study carried out with any LPS type at 37 °C. The use of this human physiological temperature is a key issue because of the considerable influence that temperature may have on the formation of LPS supramolecular aggregates.[11]

Aurell and Wistrom[12] used a rather indirect experimental technique that involved fluorescence spectroscopy of mixed micelles of LPS and a fluorescent probe and suggested a change in the aggregation of the LPS from *E. coli* serotype 026:B6 at $c = 14$ μg mL^{-1} at 25 °C. This value is identical to the CMC$_a$ obtained by us at 37 °C, both by static and dynamic light scattering spectroscopy.

Static light scattering data allow calculation of the M_w, A_2, and R_g values, both below and above the CMC$_a$ (Table 1). Moreover, the CMC$_a$ value itself could be determined. The M_w value obtained below the CMC$_a$ represents either the effective molecular weight of the monomer or the presence of LPS dimers or higher-order oligomers even below the CMC$_a$ (premicelle oligomers). The M_w value obtained above the CMC$_a$ is (approximately) three times that obtained below the CMC$_a$, which suggests the formation of trimers of the units present below the CMC$_a$. Moreover, the M_w value below the CMC$_a$ is considerably higher than those obtained for other LPS types (summarized by Aurell and Wistrom[12]). Both observations strongly suggest that LPS is dispersed in premicelle oligomers below the CMC$_a$. The M_w value calculated for the LPS aggregates is of the same magnitude as those indicated for the aggregates of other LPS types.[13, 14]

Based on thermodynamics, the negative second virial coefficient values obtained indicate a poor interaction between LPS and the aqueous solvent (that is, a tendency towards self-association). The increase of the A_2 value above the CMC$_a$ indicates a better interaction with the solvent, possibly as a result of the expected (better) shielding of LPS hydrophobic components from the aqueous environment and increase of the intermolecular interactions upon micelle formation.

The diameters obtained by dynamic light scattering spectroscopy for the LPS aggregates from *E. coli* serotype 026:B6 at 37 °C are higher than the values obtained for other LPS types at room temperature with the same technique[14, 15] as well as by microscopy imaging methods.[13, 15] The data presented in Figure 4 indicates that well above the CMC$_a$, the increase of LPS concentration results in more aggregates, without any change in their dimensions. The apparent transition range and the hyperbolic-like distribution of the data points arise from the coexistence of two supramolecular species, which leads to an apparent intermediate diameter and to asymptotic behavior (Figure 4) as a result of a balance of the light scattering contributions from the premicelle oligomers and from the larger aggregates in the calculations of the average diffusion coefficient (and thus, the average diameter).

The value of $\rho = 0.86$ obtained below the CMC$_a$ is in agreement with a nearly spherical geometry, when the increase in ρ values to be expected for polydisperse samples is considered (Figure 3). The change in this parameter observed above the CMC$_a$ indicates a different aggregate geometry at those concentrations. Theoretical equations[16, 17] can be used to estimate R_g and R_h values (and, therefore, ρ) if geometry and dimensions are known. However, the geometry and axial dimensions published by Aurell et al.[15] lead to estimates that are not in agreement with our experimental results. However, comparison of the two studies is hampered by the fact that different LPS types and temperatures were used. Moreover, no indication of the aggregation state of the sample (namely, below or above the CMC$_a$) is provided by Aurell et al.[15].

There is a possible correlation between our findings and the LPS concentration-dependent physiological functional effects, which could be explained by a better accessibility of recognition structures to CD14 and/or LBP (LPS-binding proteins required for cell activation) in the smaller premicelle oligomers. This hypothetical differential accessibility can be simply related to the difference between the surface curvature of the two supramolecular structures. Our data indicates that (within the studied concentration range) there are no significant concentration-dependent alterations of the dimensions of the supramolecular structures below the CMC_a (only a decrease in the number of aggregates). Concentration-dependent decrease in endotoxin action can also be related to the variation of the maxima of the size distributions (hydrodynamic diameter) obtained by dynamic light scattering (Figure 4) and to the difference between the A_2 values obtained below and above the CMC_a (different solvent interactions). A full characterization of the binding of LBP and CD14 to the different LPS supramolecular structures (similar to the study carried out by Tobias et al.[14]) will be essential to further evaluate this hypothesis. A future characterization of the aggregation of biologically active rough mutant LPS could also further clarify this idea.

The combination of static and dynamic light scattering spectroscopy enables direct characterization of the LPS aggregation process. Our data strongly suggest that future in vitro studies with LPS strains should be carried out both below and above their CMC_a (14 μg mL^{-1} for this strain) in order to distinguish between the pathological effects caused by LPS large aggregates and those caused by the premicelle oligomers. Future research should be carried out to study the molecules that influence the LPS aggregation process and thus control partition of LPS in the bloodstream. The results presented open new perspectives for alternative therapeutic strategies. The search for drugs that interact with the aggregates and change the CMC_a value could be a new way to overcome certain bacterial-endotoxin-related pathologies.

Methods

Apparatus: In light scattering experiments, light from a laser impinges on the scattering sample and is partially scattered. The position of a detector defines the scattering angle (θ) and scattering volume (Figure 5). Light scattering measurements were carried out in a BI-2030AT apparatus with a 128-channel digital autocorrelator (Brookhaven Instruments Corporation, Holtsville, NY, USA), equipped with a Spectra-Physics He – Ne Laser, model 127 (632.8 nm, 35 mW).

Static light scattering: Static light scattering (SLS) measurements were carried out using the Zimm method[18] in order to obtain R_g, M_w, and A_2 values. The statistical weighting of these average values was previously described.[19] The Zimm method is based on the following equation:

$$\frac{K \times c}{R_\theta} = \left(1 + \frac{16\pi^2 n_0^2 R_g^2}{3\lambda^2}\sin^2\left(\frac{\theta}{2}\right)\right)\left(\frac{1}{M_w} + 2A_2\right) \quad (1)$$

where c is the weight concentration, R_θ is the Rayleigh ratio (a parameter proportional to the scattering intensity, obtained by SLS for each c and θ value), n_0 is the refractive index of the solvent and K is defined by Eq. (2).

$$K = \frac{4\pi^2 n_0^2 \left(\frac{dn}{dc}\right)^2}{N_A \lambda^4} \quad (2)$$

Here, dn/dc is the specific refractive index increment of the solution, N_A the Avogadro number, and λ the wavelength of the laser. A plot of $(K \cdot c)/R_\theta$ against $\sin^2(\theta/2) + k' \cdot c$ (where k' is an arbitrary constant chosen purely for graphical convenience) gives a grid plot (Figure 6) known as the Zimm plot. This plot is made of two sets of lines, which consist of the angular measurements at each concentration and the concentration measurements at each θ value. Extrapolation of the angular and concentration measurements to zero gives the values of A_2, R_g, and M_w. Our measurements were carried out at scattering angles from 45 – 150°. The experimental determination of dn/dc, was hampered by the need for considerably higher LPS concentrations. Thus, a value of dn/dc = 0.15 cm^3 g^{-1} was used in the present work, as previously determined for several polysaccharides and phospholipids in aqueous solution or suspension.[20]

A simplification of the Zimm method, called the Debye method, was also used to determine the CMC_a. The scattering intensities were

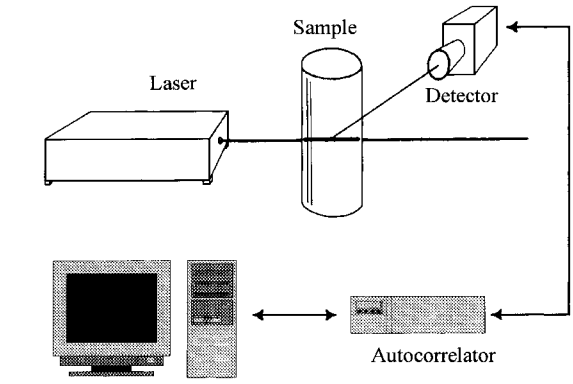

Figure 5. *Schematic representation of the light scattering apparatus. The detector is mounted on a goniometer in order to carry out the scattering intensity measurements at different scattering angles. The presence of the autocorrelator is only necessary for pretreatment of the dynamic light scattering data (in order to obtain the intensity correlation functions).*

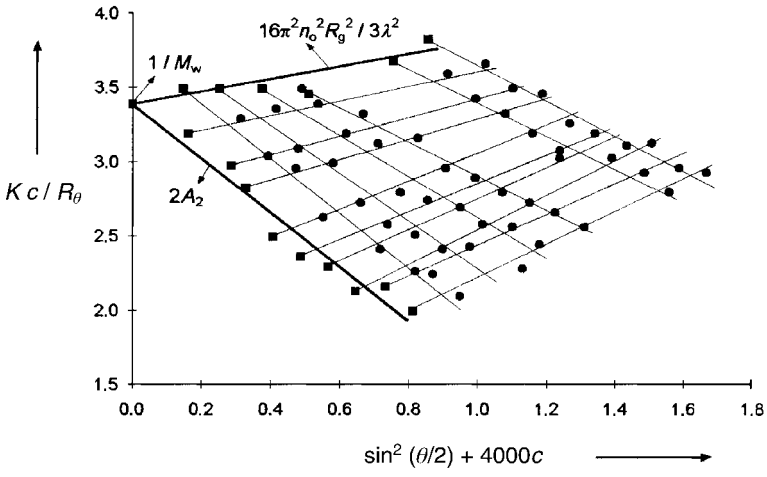

Figure 6. *Zimm plot. The extrapolated lines used for the calculation of each static light scattering parameter are indicated.*

measured at $\theta = 90^\circ$ for a range of concentrations that included the CMC_a and the values obtained were used to produce a $(K \cdot c)/R_\theta$ versus c plot. In accordance with Eq. (3), the different A_2 and M_w values found below and above the CMC_a lead to the occurrence of two straight lines.

$$\frac{K \times c}{R_\theta} = \frac{1}{M_w} + 2A_2c \quad (3)$$

The value of the CMC_a is indicated by the concentration at the intersection of the two lines generated by the plot.

Dynamic light scattering: DLS techniques provide information on the dynamical properties of the scattering molecules or aggregates on a microsecond time scale by performing an autocorrelation with the scattering intensity data. As long as the scattered field time function is Gaussian, the intensity correlation function obtained, $g_2(t)$, is related to the field correlation function $g_1(t)$ by the Siegert equation,[16]

$$g_2(t) = 1 + \beta g_1(t) \quad (4)$$

where β is a constant (ideally $\beta = 1$). For small particles or spheres of any size,

$$g_1(t) = e^{-\Gamma t} \quad (5)$$

$$\Gamma = Dq^2 \quad (6)$$

$$q = \frac{4\pi n_0}{\lambda} \sin\frac{\theta}{2} \quad (7)$$

D is the translational diffusion coefficient. For diluted solutions (such as those used in the present work), D can be used to calculate the hydrodynamic radius, R_h, by using the Stokes – Einstein equation,

$$D \approx \frac{kT}{6\pi\eta R_h} \quad (8)$$

where k is the Boltzmann constant, T the absolute temperature, and η the solvent viscosity.

Since we are dealing with polydisperse samples, the size distributions of the samples were obtained by using the standard CONTIN method,[9] considered to be the most suitable approach for the study of systems with broad size distributions (its potentialities and drawbacks were tested and reviewed by Johnsen and Brown[21]).

Static and dynamic light scattering information were combined to calculate the value of ρ:[22]

$$\rho = \frac{R_g}{R_h} \quad (9)$$

This value is a structure-dependent parameter, which usually varies from 0.775 for a homogeneous sphere (lower values are also possible) to $\rho > 2.0$ for long rigid rods (a complete set of ρ values and equations according to specific structures was presented by Burchard[23]).

Sample preparation: All the laboratory material used for the preparation of light scattering samples was treated with a chromo-sulfuric mixture (in order to remove lipids or other traces that can retain "dust" particles on the material inner surfaces) and thoroughly rinsed with distilled water, previously filtered through 0.2 μm cellulose nitrate membranes (MFS, Dublin, CA, USA). Samples were prepared in a syringe and filtered through Millipore Millex-HV 0.8-μm disposable filter units directly into cylindrical light-scattering tubes. To remove the remaining "dust" particles (which could lead to biased light scattering results), an additional mild centrifugation (45 min, 1300 g) was performed to sediment the particles in the bottom of the cell. Afterwards, the tubes were handled with extreme care.

In the present study, we used 18 different concentrations of lipopolysaccharide from *Escherichia coli* serotype 026:B6 (Sigma, St. Louis, MO, USA), in the range 1 – 100 μg mL^{-1}. These solutions (suspensions) were prepared in Dulbecco's PBS, pH 7.4, from a 100-μg mL^{-1} stock solution. All the measurements were carried out at 37 °C.

This work was supported by Fundação para a Ciência e Tecnologia and by Fundação Calouste Gulbenkian (Portugal).

[1] G. Majno, I. Joris, *Cells, Tissues and Disease: Principles of General Pathology*, Blackwell, Cambridge, **1996**.

[2] E. T. Rietschel, T. Kirikae, F. U. Schade, U. Mamat, G. Schmidt, H. Loppnow, A. J. Ulmer, U. Zähringer, U. Seydel, F. Di Padova, M. Schreier, H. Brade, *FASEB J.* **1994**, *8*, 217 – 225.

[3] D. J. Shaw, *Introduction to Colloid and Surface Chemistry, 4th ed.*, Butterworth Heinemann, Woburn, **1992**.

[4] a) N. J. Turro, A. Yekta, *J. Am. Chem. Soc.* **1978**, *100*, 5951 – 5952; b) F. Grieser, C. J. Drummond, *J. Phys. Chem.* **1988**, *92*, 5580 – 5593; c) P. J. Tummino, A. Gafni, *Biophys. J.* **1993**, *64*, 1580 – 1587.

[5] C. Y. Young, P. J. Missel, N. A. Mazer, G. B. Benedek, M. C. Carey, *J. Phys. Chem.* **1978**, *82*, 1375 – 1378.

[6] P. J. Missei, N. A. Mazer, G. B. Benedek, C. Y. Young, M. C. Carey, *J. Phys. Chem.* **1980**, *84*, 1044 – 1057.

[7] J. P. Kratohvil, *J. Colloid Interface Sci.* **1980**, *75*, 271 – 275.

[8] a) E. Ruckenstein, R. Nagarajan, *J. Colloid Interface Sci.* **1976**, *57*, 388 – 390; b) M. G. Neumann, M. H. Gehlen, *J. Colloid Interface Sci.* **1990**, *135*, 209 – 217.

[9] a) S. W. Provencher, *Comput. Phys. Commun.* **1982**, *27*, 213 – 227; b) S. W. Provencher, *Comput. Phys. Commun.* **1982**, *27*, 229 – 242.

[10] D. E. Koppel, *J. Chem. Phys.* **1972**, *57*, 4814 – 4820.

[11] a) K. Brandenburg, A. Blume, *Thermochim. Acta* **1987**, *119*, 127 – 142; b) K. Brandenburg, U. Seydel, *Biochim. Biophys. Acta* **1991**, 1069, 1 – 4; c) S. Srimal, N. Surolia, S. Balasubramanian, A. Surolia, *Biochem. J.* **1996**, *315*, 679 – 686.

[12] C. A. Aurell, A. O. Wistrom, *Biochem. Biophys. Res. Commun.* **1998**, *253*, 119 – 123.

[13] M. J. Gould, M. E. Dawson, T. J. Novitsky, *Part. Sci. Technol.* **1991**, *9*, 55 – 59.

[14] P. S. Tobias, K. Soldau, N. M. Iovine, P. Elsbach, J. Weiss, *J. Biol. Chem.* **1997**, *272*, 18682 – 18685.

[15] C. A. Aurell, M. E. Hawley, A. O. Wiström, *Mol. Cell Biol. Res. Commun.* **1999**, *2*, 42 – 46.

[16] B. J. Berne, R. Pecora, *Dynamic Light Scattering*, Robert E. Krieger Pub. Co., Malabar, **1990**.

[17] K. S. Schmitz, *Dynamic Light Scattering by Macromolecules*, Academic Press, San Diego, **1990**.

[18] B. H. Zimm, *J. Chem. Phys.* **1948**, *16*, 1099 – 1116.

[19] N. C. Santos, M. A. R. B. Castanho, *Biophys. J.* **1996**, *71*, 1641 – 1650.

[20] a) M. B. Huglin in *Polymer Handbook* (Eds.: J. Brandrup, E. H. Immergut), John Wiley, New York, **1989**, pp. VII/409 – 484; b) C. S. Chong, K. Colbow, *Biochim. Biophys. Acta* **1976**, *436*, 260 – 282.

[21] R. Johnsen, W. Brown, in *Laser Light Scattering in Biochemistry* (Eds.: S. E. Harding, D. B. Sattelle, V. A. Bloomfield), The Royal Society of Chemistry, Cambridge, **1992**, pp. 77 – 91.

[22] a) N. C. Santos, M. J. E. Prieto, A. Morna-Gomes, D. Betbeder, M. A. R. B. Castanho, *Biopolymers* **1997**, *41*, 511 – 520; b) N. C. Santos, A. M. A. Sousa, D. Betbeder, M. Prieto, M. A. R. B. Castanho, *Carbohydr. Res.* **1997**, *300*, 31 – 40.

[23] W. Burchard in *Light Scattering from Polymers* (Eds.: H.-J. Cantow, G. Dall'Asta, K. Dušek, J. D. Ferry, H. Fujita, M. Gordon, J. P. Kennedy, W. Kern, S. Okamura, C. G. Overberger, T. Saegusa, G. V. Schulz, W. P. Slichter, J. K. Stille), Springer-Verlag, Berlin, **1983**, pp. 1 – 124.

Received: July 26, 2002 [F 462]